

# Dimensionless and analytical studies of the thermal stability of a high temperature superconducting tube

J. Lévêque \*, A. Rezzoug

*GREEN-UHP, Faculte des Sciences, University of Nancy, BP 239, F-54506 Vandoeuvre-lès-Nancy, France*

Received 20 September 2002; received in revised form 14 February 2005

## Abstract

This paper deals with the influence of thermal conductivity and specific heat on the stability of a superconducting tube. The study is made to foresee the effect of a pulse of energy, which causes the quench of the superconductor. Depending on the applications, the transition of the superconductor is provoked, like for the superconducting current limiter, or accidental. In any case, it is necessary to protect the superconductor from an excessive rise of temperature to avoid its destruction. Using dimensionless analysis, the study is applied to a cylindrical tube.

© 2005 Published by Elsevier Ltd.

*Keywords:* High  $T_c$  superconductor (A); Stability (C); Heat Transfer (C)

## 1. Introduction

Superconductors are characterised by two fundamental properties, they have no resistance and are perfectly diamagnetic. This diamagnetism allows to expel or to trap magnetic field. These properties exist only under some conditions on temperature  $T$ , magnetic field  $H$  and current density  $J$ . In this 3-D space, three critical values  $T_c$ ,  $H_c$  and  $J_c$ , define a critical surface for a given material. This material is in superconducting state if, and only if, its functioning point is located under the so defined surface.

When a local energy is supplied in a superconducting material, its temperature increases. If the temperature

rise is sufficient, a part of the superconductor becomes resistive. Therefore, two cases are to be considered: either the normal zone vanishes and the system is stable or it expands to the whole system and the system is unstable. This transition could be useful in some uses to limit the current or to give a pulse of energy, but it must be avoided in other applications. Whatever the application, the study of the transition is necessary to prevent an excessive temperature rise of the superconductor for fear of destruction.

High critical temperature materials, which appear in 1986, will be used, without any doubt, in many areas, and especially in electrical engineering. Today, those new materials are mainly ceramics and can be used, in some applications, under a bulk shape.

To contribute to the expansion of this material, besides theoretical studies, engineering tools have to be developed to help the designer of such apparatus. This paper is a contribution to the study of the important problem of the stability of the bulk superconductor.

\* Corresponding author. Tel.: +33 3 83 68 41 25; fax: +33 3 83 68 41 85.

*E-mail address:* [jean.leveque@green.uhp-nancy.fr](mailto:jean.leveque@green.uhp-nancy.fr) (J. Lévêque).

The study presented here concerns the influence of the geometrical and physical parameters on the stability of a tube shaped superconductor. This form is used in many applications like current lead or cylindrical current limiter.

Taking into account the fixed goal, we have to set methods in which the parameters appear explicitly. To do that, we set some hypothesis to simplify the models.

The methods presented as well as the numerical results could be extended to other superconducting material or to other shapes.

The paper is divided into three main parts; the first one is devoted to the model, the hypothesis and the analytical solutions. Numerical results are developed in the second part. The variations of the physical parameters with the temperature are presented in the last part.

## 2. Modelling

The studied system is a tube made of a bulk superconducting material and usually used as a current lead. All the geometrical parameters are reported in Fig. 1. Of course, because of the shape, cylindrical co-ordinates are used to set the mathematical model.

We study the behaviour of this tube when an energy pulse is applied for a short time in a small zone in its thickness. The considered impulsion can be provoked by an extra current, by a shock or by a structure default.

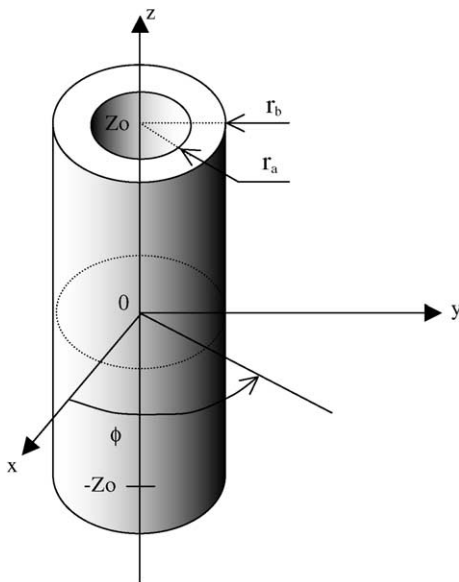


Fig. 1. Representation of the tube.

### 2.1. Limits of the study and assumptions

The study will be limited to a short time following the pulse application, this time is sufficient to know if the system goes to a stable state or not. The shortness of the time implies that the heat cannot diffuse to the borders of the tube, so the temperature can be considered as adiabatic on the walls. So, the conditions of the study are the followings:

- $T = T_{\text{bath}}$  for the whole tube at  $t = 0$ .
- $\frac{\partial T}{\partial n} = 0$  on the boundaries  $\forall t$  (1)
- The current in the tube is constant because it is usually imposed by an external source.
- Only the own field of the tube is considered to the exclusion of any other external field.

### 2.2. Heat transfer

Temperature distribution  $T(r, \theta, z, t)$  is governed by heat transfer equation:

$$C_p \frac{\partial T}{\partial t} = \text{div}(\overline{\overline{\lambda}} \nabla(T)) + P \tag{2}$$

where  $P$  is an internal source, which is the power dissipated by Joule effect ( $\text{W m}^{-3}$ ),  $C_p(T)$  is the specific heat ( $\text{J m}^{-3} \text{K}^{-1}$ ),  $\overline{\overline{\lambda}}(T)$  is the tensor of the thermal conductivity ( $\text{W m}^{-1} \text{K}^{-1}$ ).

To simplify this tensor, radial and axial thermal conductivities are expressed as functions of the azimuthal component of thermal conductivity. Introducing coefficients  $\alpha_r$  and  $\alpha_z$ , this tensor can be expressed as

$$\overline{\overline{\lambda}} = \begin{pmatrix} \lambda_z & 0 & 0 \\ 0 & \lambda_r & 0 \\ 0 & 0 & \lambda_\theta \end{pmatrix} = \lambda_\theta \begin{pmatrix} 1/\alpha_z & 0 & 0 \\ 0 & 1/\alpha_r & 0 \\ 0 & 0 & 1 \end{pmatrix} \tag{3}$$

In cylindrical co-ordinates, Eq. (2) becomes:

$$C_p \frac{\partial T}{\partial t} = \lambda_z \frac{\partial^2 T}{\partial z^2} + \lambda_r \left( \frac{\partial^2 T}{\partial r^2} + \frac{1}{r} \frac{\partial T}{\partial r} \right) + \frac{\lambda_\theta}{r^2} \frac{\partial^2 T}{\partial \theta^2} + P \tag{4}$$

and could be rewritten as

$$C_p \frac{\partial T}{\partial t} = \lambda_\theta \left( \frac{1}{\alpha_z} \frac{\partial^2 T}{\partial z^2} + \frac{1}{\alpha_r} \left( \frac{\partial^2 T}{\partial r^2} + \frac{1}{r} \frac{\partial T}{\partial r} \right) + \frac{1}{r^2} \frac{\partial^2 T}{\partial \theta^2} \right) + P \tag{5}$$

Now, we introduce a coefficient  $\alpha_{cp}$ . Thanks to this coefficient, we are able to vary the specific heat around a prescribed value. So, the last equation is rewritten as following:

$$\alpha_{cp} C_p \frac{\partial T}{\partial t} = \lambda_\theta \left( \frac{1}{\alpha_z} \frac{\partial^2 T}{\partial z^2} + \frac{1}{\alpha_r} \left( \frac{\partial^2 T}{\partial r^2} + \frac{1}{r} \frac{\partial T}{\partial r} \right) + \frac{1}{r^2} \frac{\partial^2 T}{\partial \theta^2} \right) + P \tag{6}$$

To solve this equation an analysis of the dissipation power is necessary.

**2.3. Dissipated power**

Dissipation term  $P$  can be shared in two terms:

- $P_j$ , due to the Joule effect when the superconductor quenches,
- $P_p$ , due to the heater pulse.

Several models exist to describe the power dissipation due to the Joule effect in a high temperature superconductor, as we can see in Fig. 2.

The simulating model is issued from some simulation of losses in high temperature superconducting material. This model is not suitable to have an analytical solution of Eq. (6).

Using Bean’s model,  $P_j$  can be expressed under two forms depending on the temperature of the superconductor:

$$\begin{cases} P_j = P_{jc} = \rho_{cl} J_s^2 & \text{if } T > T_c \\ P_j = 0 & \text{if } T < T_c \end{cases}$$

Unfortunately, this kind of step function is not suitable to solve analytically Eq. (6).

To do that, we suggest to adopt a linear function  $P_j(T)$ , the slope of this one is called  $\Delta$ .

At first sight, this approximation seems to be a strong hypothesis and needs explanations. The adopted model is based on the conservation of the average dissipated power compared to the Bean’s model. To respect that, slope  $\Delta$  is chosen so as the hatching areas in Fig. 2 becomes equal. With this condition, the average power is independent between this model and Bean’s model. Like in the simulating model, the power begins to be dissipated at the bath temperature. So, our model is intermediate between Bean’s and simulating model.

The second part of dissipation term,  $P_p$ , is the external energy supplied to the superconductor. To start the quench, we consider a given energy  $E_p$  distributed on a small zone  $V(r, \theta, z, t)$  of the tube for a time  $t$ . So the specific energy distributed is given as:

$$P(r, \theta, z, t) = E_p J(V(r, \theta, z, t)).$$

**2.4. Method of resolution**

Taking into account the two parts of the dissipation term, Eq. (6) is rewritten as follows:

$$\frac{\mu C_p \alpha_{cp}}{\lambda_\theta} \frac{\partial T}{\partial t} = \frac{1}{\alpha_z} \frac{\partial^2 T}{\partial z^2} + \frac{1}{\alpha_r} \left( \frac{\partial^2 T}{\partial r^2} + \frac{1}{r} \frac{\partial T}{\partial r} \right) + \frac{1}{r^2} \frac{\partial^2 T}{\partial \theta^2} + \frac{\Delta}{\lambda_\theta} (T - T_{\text{bath}}) + \frac{P_p(r, \theta, z, t)}{\lambda_\theta} \tag{7}$$

with  $C_p$  the specific heat and  $\mu$  the density.

To solve this equation independently of the sizes of the tube, we introduce dimensionless variables as follow:

$$\begin{cases} r_1 = \frac{r}{r_b} \\ r_{ab} = \frac{r_b - r_a}{r_b} \\ z_1 = \frac{z}{z_0} \\ \Theta = \frac{T - T_b}{T_0 - T_b} \end{cases}, \begin{cases} \tau = t \frac{\lambda_\theta}{\mu C_p r_b^2} \\ \Phi_j = \frac{\Delta}{\lambda_\theta} r_b^2 \\ \Phi_p \cdot f(\tau) = \frac{r_b^2}{\lambda_\theta (T_c - T_{\text{bath}})} P_p(r, \theta, z, t) \\ \text{with } P_p(r, \theta, z, t) = P_p \cdot f(r, \theta, z, t) \end{cases} \tag{8}$$

We notice that dimensionless power,  $\Phi_j$ , depends on  $r_b$ .

To give a simple form to the equation, we remove all the subscripts. So, using the previous dimensionless variable, with the following notations,  $r, z, \theta$ , and  $\tau$ , Eq. (7) becomes:

$$\frac{\partial \Theta}{\partial \tau} = \frac{1}{\alpha_z} \frac{\partial^2 \Theta}{\partial z^2} + \frac{1}{\alpha_r} \left( \frac{\partial^2 \Theta}{\partial r^2} + \frac{1}{r} \frac{\partial \Theta}{\partial r} \right) + \frac{1}{r^2} \frac{\partial^2 \Theta}{\partial \theta^2} + \Phi_j \Theta + \Phi_p \cdot f(r, \theta, z, \tau) \tag{9}$$

To suppress the term depending on  $\Theta$  in Eq. (9), we set a last change of variable:

$$\Theta(r, \theta, z, \tau) = \tilde{\Theta}(r, \theta, z, \tau) e^{\alpha \tau} \tag{10}$$

Replacing  $\Theta$  by its expression, gathering the time dependant terms and dividing by the exponential, Eq. (9) becomes:

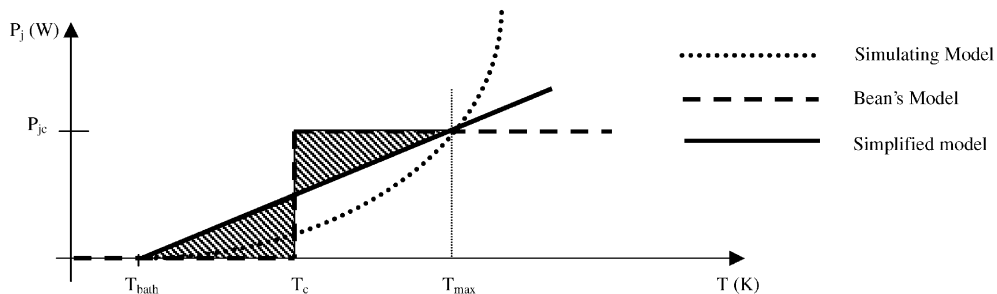


Fig. 2. Representation of Joule effect losses.

$$\alpha_{cp} \frac{\partial \tilde{\Theta}}{\partial \tau} = \frac{1}{\alpha_z} \frac{\partial^2 \tilde{\Theta}}{\partial z^2} + \frac{1}{\alpha_r} \left( \frac{\partial^2 \tilde{\Theta}}{\partial r^2} + \frac{1}{r} \frac{\partial \tilde{\Theta}}{\partial r} \right) + \frac{1}{r^2} \frac{\partial^2 \tilde{\Theta}}{\partial \theta^2} + e^{-\alpha z} \Phi_p f(r, \theta, z, \tau) + (\Phi_j - \alpha \alpha_{cp}) \tilde{\Theta} \quad (11)$$

Until now  $\alpha$  is arbitrary, we choose  $\alpha = \Phi_j/\alpha_{cp}$  to suppress the last term and obtain:

$$\alpha_{cp} \frac{\partial \tilde{\Theta}}{\partial \tau} = \frac{1}{\alpha_z} \frac{\partial^2 \tilde{\Theta}}{\partial z^2} + \frac{1}{\alpha_r} \left( \frac{\partial^2 \tilde{\Theta}}{\partial r^2} + \frac{1}{r} \frac{\partial \tilde{\Theta}}{\partial r} \right) + \frac{1}{r^2} \frac{\partial^2 \tilde{\Theta}}{\partial \theta^2} + e^{-\frac{\Phi_j}{\alpha_{cp}} z} \Phi_p f(r, \theta, z, \tau) \quad (12)$$

Eq. (11) is solved thanks to an integral transform [1]. The solution is obtained under a series form:

$$\tilde{\Theta}(r, \theta, z, \tau) = \sum_p \sum_v \sum_m \frac{Z(\eta_p, z)}{N_z} \frac{R_v(\beta_m, r)}{N_v(\beta_m)} \frac{1}{\gamma \pi} \times \left\{ \frac{1}{\alpha_{cp}} e^{-(\eta_p^2 + \beta_m^2) \tau / \alpha_{cp}} \times \left\{ \int_0^{\tau} g'''(\eta_p, \beta_m, v, t') e^{-(\eta_p^2 + \beta_m^2) t' / \alpha_{cp}} dt' \right\} \right\} \quad (13)$$

with

$$\begin{aligned} & \int_0^{\tau} g'''(\eta_p, \beta_m, v, t') e^{-(\eta_p^2 + \beta_m^2) t' / \alpha_{cp}} dt' \\ &= \int_{-z_p}^{+z_p} Z(\eta_p, z') dz' \int_{r_{pa}}^{r_{pb}} r' R_v(\beta_m, r') dr' \\ & \times \int_{-\theta_p}^{+\theta_p} \cos(v(\theta - \theta')) d\theta' \\ & \times \int_0^{\tau} \Phi_p e^{-\Phi_j t'} e^{-(\eta_p^2 + \beta_m^2) t' / \alpha_{cp}} dt \end{aligned} \quad (14)$$

The terms of the solution can be detailed along each axis as follows:

- For the  $z$ -axis:

$$N_z = \frac{1}{2z_o} \quad \eta_p = p \frac{\pi}{z_o} \quad \text{and} \quad Z(\eta_p, z) = \cos(\eta_p \sqrt{\alpha_z z}) \quad (15)$$

- For the  $r$ -axis:

$$\frac{1}{N_v(\beta_m)} = \frac{\pi^2}{2} \frac{\alpha_r J_{v\sqrt{\alpha_r}}^2(\sqrt{\alpha_r} r_{ab} \beta_m) \beta_m^2}{J_{v\sqrt{\alpha_r}}^2(\sqrt{\alpha_r} r_{ab} \beta_m) - J_{v\sqrt{\alpha_r}}^2(\sqrt{\alpha_r} \beta_m)} \quad (16)$$

$$\begin{aligned} R_v(\beta_m, r) &= J_{v\sqrt{\alpha_r}}(\sqrt{\alpha_r} r \beta_m) Y_{v\sqrt{\alpha_r}}(\sqrt{\alpha_r} \beta_m) \\ & - J_{v\sqrt{\alpha_r}}(\sqrt{\alpha_r} \beta_m) Y_{v\sqrt{\alpha_r}}(\sqrt{\alpha_r} r \beta_m) \end{aligned} \quad (17)$$

with  $\beta_m$  the solution of:

$$\begin{aligned} & J_{v\sqrt{\alpha_r}}(\sqrt{\alpha_r} r_{ab} \beta_m) Y_{v\sqrt{\alpha_r}}(\sqrt{\alpha_r} \beta_m) \\ & - J_{v\sqrt{\alpha_r}}(\sqrt{\alpha_r} \beta_m) Y_{v\sqrt{\alpha_r}}(\sqrt{\alpha_r} r_{ab} \beta_m) = 0 \end{aligned} \quad (18)$$

where  $J_v, Y_v$  are elliptic functions.

- For the  $\theta$ -axis:

$$\gamma = 1 \text{ if } v \neq 0 \quad \text{and} \quad 2 \text{ if } v = 0 \quad (19)$$

To achieve the solution, the term number of the series is the result of a compromise between a good precision along each direction and a reasonable time of computation. After trials, 19 terms have been chosen.

### 3. Numerical results

At first, we define a reference system, after that we study the effect of a variation of the physical parameters on this system. Subsequently, we study the influence of the dissipated power.

#### 3.1. Reference system

Considering a high temperature superconducting material, such as YBCO and BSCCO, the specific heat and the thermal conductivity respectively vary between  $10^5$  and  $10^7 \text{ J/m}^{-3} \text{ K}^{-1}$  and  $0.5\text{--}50 \text{ W m}^{-1} \text{ K}^{-1}$ . We have chosen a medium of those usual values.

The range of variation of the physical parameters is defined by coefficients  $\alpha_r, \alpha_z$  and  $\alpha_{cp}$  that appear in the heat transfer equation. The same value is chosen for radial and axial conductivity, so  $\alpha_r = \alpha_z$ .

All the characteristics of the studied system are summarised in the Table 1.

The external radius,  $r_{bs}$  of the tube being fixed, we remember that in Eq. (8) the initial power pulse depends on this radius, and so the main study depends on this choice. To determine the initial power and the Joule effect dissipation, we used the parameters of Table 2, these values are usual.

The dimensional duration of the heat power pulse is  $\tau = 0.025$ . Depending on the kind of physical parameters, this time is sufficient to obtain a rise in temperature situated between 100 K and 200 K. To achieve the

Table 1  
Characteristics of the studied system

|                               |                           |  |
|-------------------------------|---------------------------|--|
| Physical reference parameters | $\lambda_{ref}$           | $5 \text{ W m}^{-1} \text{ K}^{-1}$    |
|                               | $C_{ref}$                 | $10^6 \text{ J m}^{-3} \text{ K}^{-1}$ |
| Physical parameters           | $\alpha_r$ and $\alpha_z$ | Between 0.1 and 10                     |
|                               | $\alpha_{cp}$             | Between 0.25 and 10                    |
| Geometrical parameters        | $r_{ab}$                  | Between 0 and 1                        |
|                               | $z_o$                     | Between 0.25 and 5                     |
|                               | $r_b$                     | 0.01 m                                 |
| Electrical parameters         | $J$                       | $10^7 \text{ A m}^{-2}$                |
|                               | $\sigma$                  | $10^{-5} \Omega \text{ m}$             |
| Dimensionless parameters      | $\Phi_j$                  | 133.3                                  |
|                               | $\Phi_p$                  | 200 000                                |
|                               | $\tau$                    | 0.025                                  |
|                               | $\tau_p$                  | 0.0025                                 |

Table 2  
Variation of the power dissipation

|                                  |        |        |          |
|----------------------------------|--------|--------|----------|
| $J$ ( $A\ m^{-2}$ )              |        | $10^7$ |          |
| $\sigma$ ( $\Omega\ m$ ) $^{-1}$ |        | $10^5$ |          |
| $r_b$ (m)                        | 0.001  | 0.01   | 0.1      |
| $\Phi_j$                         | 1.33   | 133.33 | 133333.3 |
| $J$ ( $A\ m^{-2}$ )              |        | $10^7$ |          |
| $r_b$ (m)                        |        | 0.01   |          |
| $\sigma$ ( $\Omega\ m$ ) $^{-1}$ | $10^6$ | $10^5$ | $10^4$   |
| $\Phi_j$                         | 13     | 133.33 | 1333.33  |
| $\sigma$ ( $\Omega\ m$ ) $^{-1}$ |        | $10^5$ |          |
| $r_b$ (m)                        |        | 0.01   |          |
| $J$ ( $A\ m^{-2}$ )              | $10^6$ | $10^7$ | $10^8$   |
| $\Phi_j$                         | 1.33   | 133.3  | 13333.3  |

numerical solution, among the possible choices, the ratio between the small volume, where the initial power is dissipated, and the whole volume of any tube is kept constant, its value is 0.25%.

In all the cases, we impose a value for  $\alpha_{cp}$  and we increase  $\alpha_r$  from 0 to know the limit of the stability. So, below the limit value of  $\alpha_r$  the system is stable, upper it is unstable.

In a first part, we study the influence of the physical parameters on the stability versus the geometrical size of the tube. Then we study the influence of the dissipated power for a given geometrical configuration.

### 3.2. Study of the geometry

For the fixed values of  $r_{ab}$ , the obtained results are summarised in Figs. 3–7. In each figure, the curves are sketched for different values of  $z_0$ . Each curve divides the plane in two parts. The system is stable if and only if point  $(\alpha, \alpha_{cp})$  is located in the low half space. It means that, in this case, the initial normal zone vanishes.

We notice that, whatever the dimensionless internal radius of tube,  $r_{ab}$ , the stability curve is constant for a value of  $\alpha_{cp}$  lower than one. Indeed, for these values of  $\alpha_{cp}$ , the specific heat is low, and so, the system is unsta-

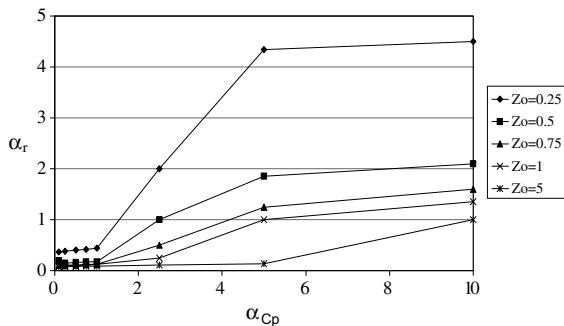


Fig. 3.  $r_{ab} = 0.05$ .

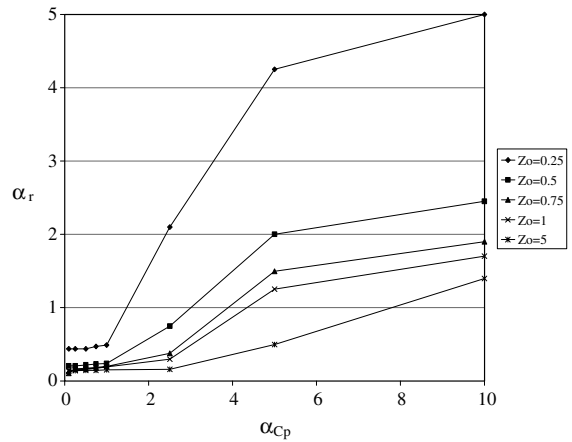


Fig. 4.  $r_{ab} = 0.25$ .

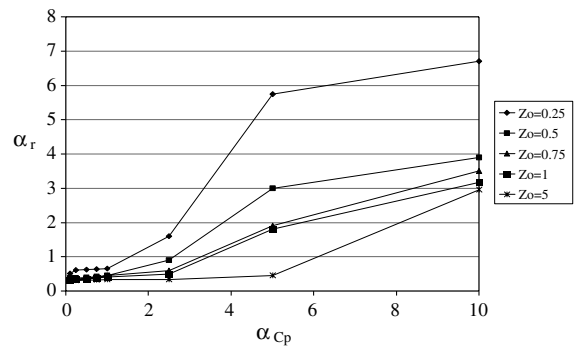


Fig. 5.  $r_{ab} = 0.5$ .

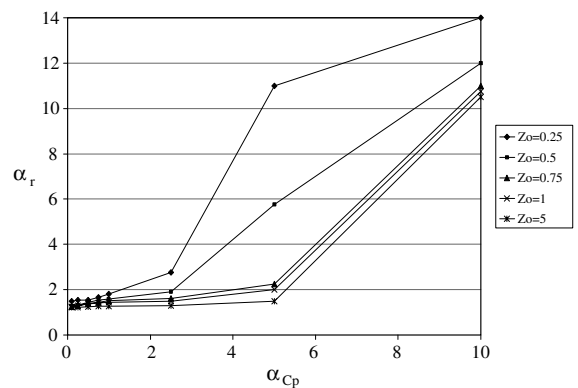


Fig. 6.  $r_{ab} = 0.75$ .

ble. We observe that for the high value of  $\alpha_{cp}$ , a superconducting tube is very stable.

One can see that stability is very difficult to obtain for a thin tube (small value of  $r_{ab}$ ), indeed the heat is transferred quickly to the whole domain and causes an important increase of temperature.

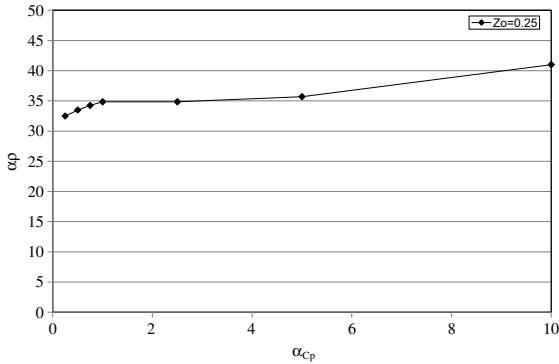


Fig. 7.  $r_{ab} = 0.95$ .

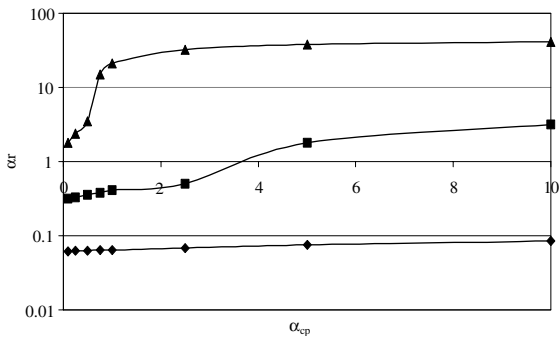


Fig. 8. Study of the influence of the power dissipated, (◆)  $\Phi_j = 666.6$ , (■)  $\Phi_j = 133.3$ , (▲)  $\Phi_j = 26.6$ .

3.3. Study of the power

The dimensionless power dissipation  $\Phi_j$  depends on  $r_b$ ,  $\sigma$ ,  $J$  and, of course, thermal conductivity. This last one is directly included in the calculus of stability. Table 2 gives some numerical results that show the effects of the variation of these parameters on the power dissipation.

To highlight the effect of the variation of the dissipation power, we have chosen to multiply and to divide Joule power dissipation,  $\Phi_j$ , by a factor five (Fig. 8).

We notice that the influence of Joule dissipation on stability is very important. Below the reference value of the electrical parameter, given in Table 1, it is very difficult to obtain a stable behaviour. Above these reference values, the tube can be considered as always stable.

4. Physical parameters

Unfortunately, the main parameters of the model depend on the temperature. So, a particular attention must be devoted to the evolution of the parameter of usual superconducting materials with the temperature. Many

results are previously presented by authors and can be found in literature. We just mention some of them in order to highlight the main characteristics that will be considered for this study.

4.1. Specific heat

From Refs. [2–4], we have extracted a set of results related to two phases of YBCO and one of BSCCO. One can see that the variations of the specific heat of the two phases of YBCO are very different (Fig. 9). For example, at a temperature of 150 K, the ratio of the values related to the phases of YBCO is about 6 and reaches 10 when the materials are different. Our presentation may be extended to a lot of high temperature superconductors. We observe that in the considered range of temperature (77 K–150 K) we do not take into account the dependence on specific heat with temperature but only an average value of it.

4.2. Thermal conductivity

Thermal conductivity also depends on the temperature and on the chosen material. In Fig. 10, the curves

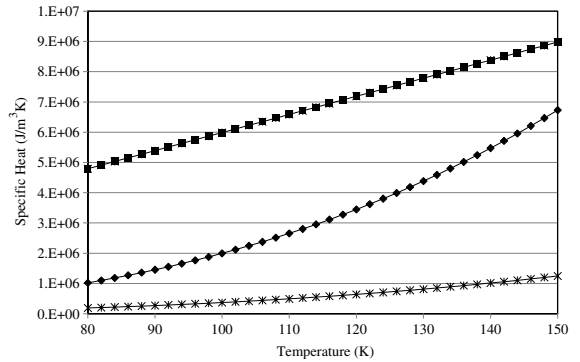


Fig. 9. Specific heat versus temperature (■)  $\text{Bi}_2\text{Sr}_2\text{CaCu}_2\text{O}_8$ , (◆)  $\text{YBa}_2\text{Cu}_4\text{O}_{8.5}$ , (\*)  $\text{YBa}_2\text{Cu}_3\text{O}_7$ .

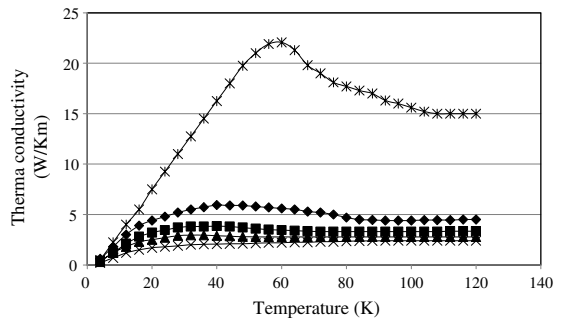


Fig. 10. Thermal conductivity of  $\text{YBa}_2\text{Cu}_3\text{O}_{7-x}$ , (◆)  $x = 0$ , (■)  $x = 0.18$ , (▲)  $x = 0.34$ , (\*)  $x = 0.48$ , (\*)  $\text{Bi}_2\text{Sr}_2\text{CaCu}_2\text{O}_8$ .

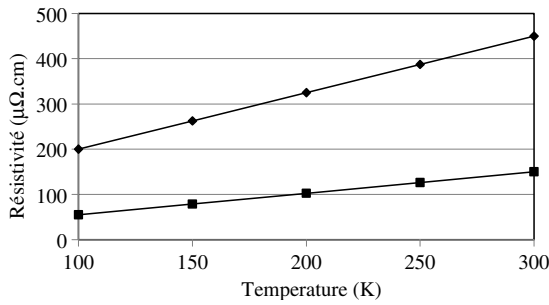


Fig. 11. Electrical resistivity of (◆) YBa<sub>2</sub>Cu<sub>3</sub>O<sub>7-δ</sub> and (■) Bi<sub>2</sub>Sr<sub>2</sub>CuO<sub>6±δ</sub> in the plan “ab” above T<sub>c</sub>.

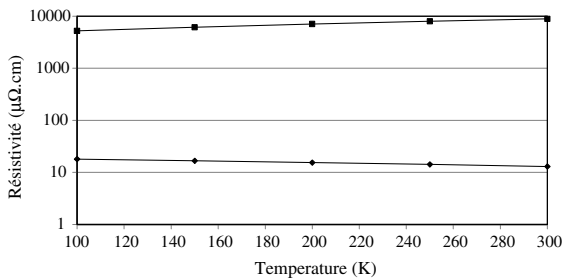


Fig. 12. Electrical resistivity of (◆) YBa<sub>2</sub>Cu<sub>3</sub>O<sub>7-δ</sub> and (■) Bi<sub>2</sub>Sr<sub>2</sub>CuO<sub>6±δ</sub> in the c-axis above T<sub>c</sub>.

characterise three phases of YBCO and one of BSCCO material. Beyond the nitrogen liquid temperature (77 K), we can notice that the value of thermal conductivity becomes roughly constant. In practice, for YBCO, we adopt a value included between 2.5 and 4.5 W m<sup>-1</sup> K<sup>-1</sup> [5–8]. Authors present many other results, in the case of BiSrCaCuO, the value of the thermal conductivity varies between 1.0 and 1.5 W m<sup>-1</sup> K<sup>-1</sup>.

### 4.3. Electrical resistivity

Above the critical temperature [2], usually, the electrical resistivity versus temperature can be expressed as:  $\rho = AT^{-1} + BT$ .

An important property of the superconducting materials is their high anisotropy in term of resistivity when plane “ab” and axis “c” are respectively considered. A ratio of 100 is not an absurd value.

Figs. 11 and 12 show the resistivity versus the temperature, for different phases of YBCO and BSCCO, respectively in plan “ab” and along c-axis.

## 5. Conclusions

A 3D model is developed to study the thermal stability of a HTS tube. Under some assumptions we can expect the behaviour of the material in terms of stability.

The obtained results show the relative influence of specific heat and thermal conductivity on thermal stability. The influence of power dissipation is also studied.

For a given tube, knowing its parameters, this study allows to delimit a functioning zone. Furthermore, the developed method or the obtained results can help to design a suitable tube for a specific apparatus, such as a current lead.

The model can be extended and applied to other shapes and apparatus using bulked or wired superconductors.

## References

- [1] N. Ozisik, Heat Conduction, John Wiley sons, 1993.
- [2] C.P. Poole, H.A. Farach, R.J. Creswick, Superconductivity, Academic press, 1995.
- [3] D. Varshney, R.K. Singh, A.K. Khaskalam, Analysis of specific heat in YBa<sub>2</sub>Cu<sub>3</sub>O<sub>7</sub>—ceramic superconductors, Phys. Status Solidi B 206 (2) (1998) 749–757.
- [4] N.E. Hussey, C.S. McMenamin, J.P. Bird, D.F. Brewer, A.L. Thomson, A.J. Young, Low temperature specific heat and thermal conductivity of high temperature superconductors, Electronic Properties and Mechanisms of High T<sub>c</sub> Superconductors, Proceedings of the International Workshop, 1998, pp. 329–331.
- [5] D. Castello, M. Jaime, M. Nunez Regueiro, C. Fainstein, Thermal conductivity of high temperature superconductors, Proceedings of the ICTPS'90 Conference on Transport Properties of Superconductors, Singapore.
- [6] F.G. Aliev, V.V. Moshchalkov, V.V. Pryadun, Thermal conductivity of the Bi<sub>2</sub>(Ca<sub>0.5</sub>Sr<sub>0.5</sub>)<sub>3</sub>Cu<sub>2</sub>O<sub>x</sub>, Tl<sub>2</sub>Ba<sub>2</sub>Ca<sub>2</sub>Cu<sub>3</sub>O<sub>x</sub> ceramics and GdBa<sub>2</sub>Cu<sub>3</sub>O<sub>x</sub> single crystal, Physica B 163 (1990) 647–648.
- [7] I.K. Kamilov, A.B. Battsalov, M.S. Buttaev, B.K. Chalkal'skii, Thermal conductivity of yttrium- and bismuth-based high T<sub>c</sub> ceramics, Supercond. Phys. Chem. Technol. 4 (10) (1991).
- [8] M.R. Delap, N.R. Bernhoeft, A model for the thermal conductivity of Yba<sub>2</sub>Cu<sub>3</sub>O<sub>7-d</sub>, Physica C 195 (1992) 301–306.